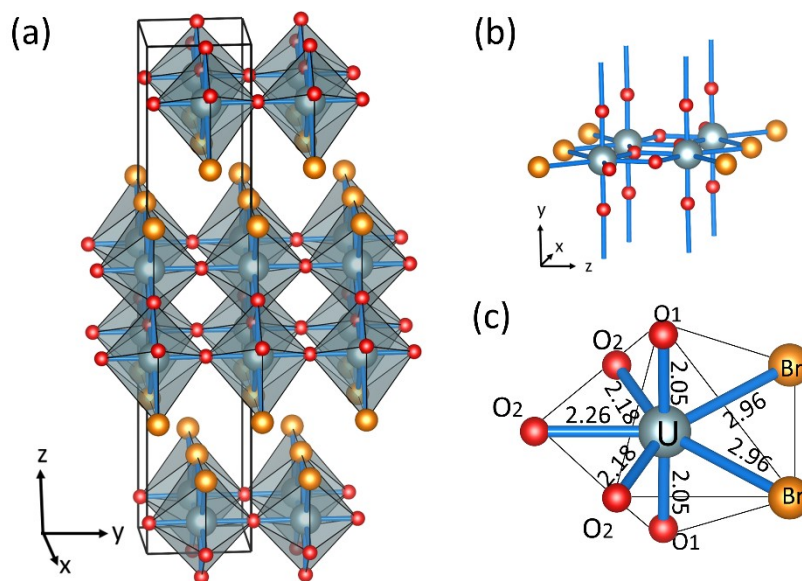


Supplementary information for “Second-order Jahn-Teller effect induced high-temperature ferroelectricity in two-dimensional NbO<sub>2</sub>X (X=I, Br)”

Huasheng Sun, Kaiming Deng, Erjun Kan\*, and Yongping Du\*

I crystal structure



**Figure S1** The layered bulk crystal structure of UO<sub>2</sub>Br.

**Calculation details on CALYPSO method:** We utilized the swarm intelligence-based CALYPSO method for global structure search, which has been successfully applied to predict a wide range of 3D and 2D structures. The structure searches for NbO<sub>2</sub>Br were carried out with simulation cells ranging from one to three formula units with 4, 8, 12 atoms respectively. Each generation contained 30 structures, and initial structures in the first generation were produced randomly with symmetry constraints. All the structures are optimized to their local minima by using density functional theory (DFT) calculations. During structure evolution, 60% of structures in the first generation with lower Gibbs free energies are selected to produce the structures in the next generation by particle swarm optimization (PSO). The other 40% was generated randomly to ensure diversity of the population. In the local optimizations, the conjugate gradient method was used and the converging criteria for the Gibbs free energy change in convective SCF steps was  $1 \times 10^{-4}$  eV per atom.

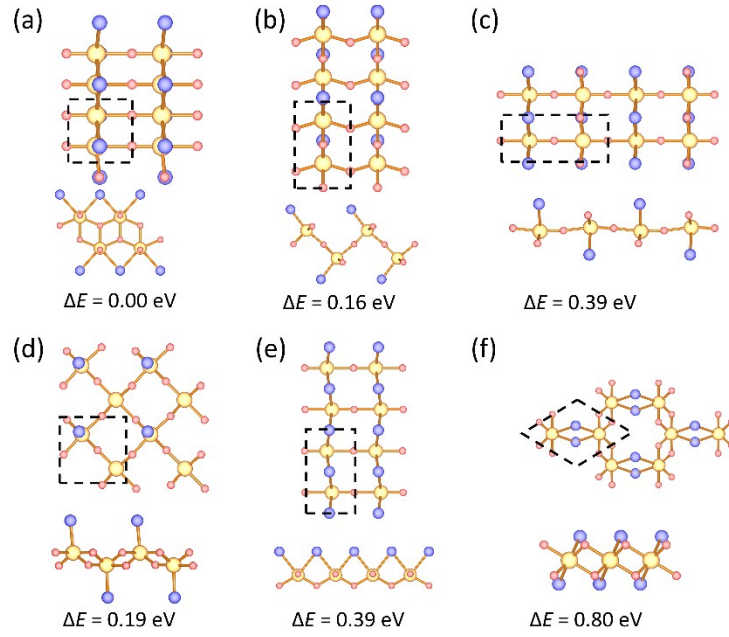


**Figure S2** Low-energy structures searched by CALYPSO and the energy differences (eV/atom) relative to ground state structure.

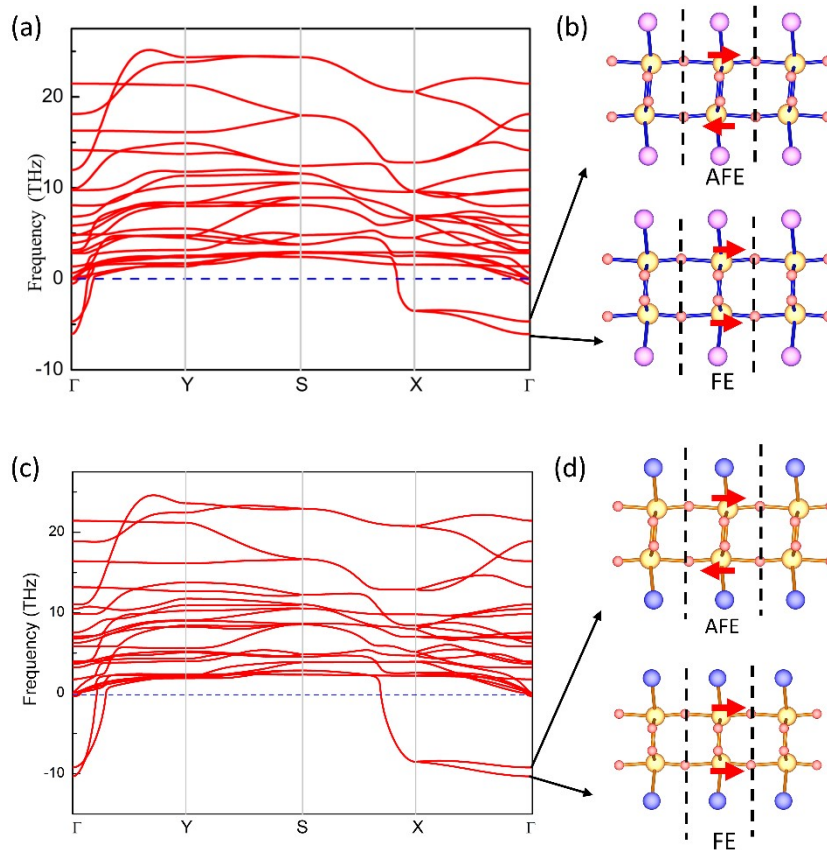


**Figure S3** Phonon spectrum for paraelectric (PE)  $\text{NbO}_2\text{X}$  monolayer. The vibrating modes of Nb atoms correspond to the imaginary frequency at the  $\Gamma$  point for the symmetric paraelectric ( $d_{2h}$ ) phase and the arrows denote the vibrating directions.

## II Ferroelectricity

The geometry of a two-dimensional NbO<sub>2</sub>X monolayer can be represented by a planar lattice consisting solely of Nb atoms. Each lattice point can be viewed as a projection of Nb ions onto a planar coordinate system. When the Nb atom is displaced from the X-axis, polarization is induced, which increases in intensity as the displacement increases. Therefore, the potential energy can be expressed in terms of the Landau-Kinzburg expansion<sup>1</sup> of order parameter  $P_i$  as:

$$E = \sum_i \left( \frac{A}{2} P_i^2 + \frac{B}{4} P_i^4 \right) + \sum_{\langle ij \rangle} \frac{C_x}{2} (P_i - P_j)^2 + \sum_{\langle ij \rangle} \frac{C_y}{2} (P_i - P_j)^2 \quad (1)$$

where the first two terms describe the FE energy for each Nb cation and parameters A and B can be obtained after fitting a double-well potential for FE NbO<sub>2</sub>X monolayers. The last two terms correspond to the interactions of  $P_i$  and  $P_j$  between two nearest neighboring Nb cations. This can be seen as the Taylor series expansion of local structural distortions, where a specific polarization is defined at each cell  $P_i$ .

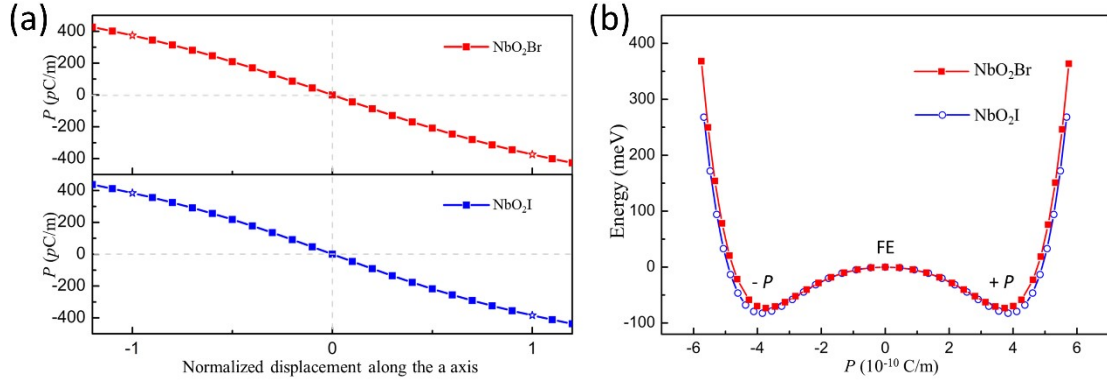


**Figure S4** (a) Calculated total polarization of NbO<sub>2</sub>X monolayer as a function of normalized displacement along the adiabatic path. The centrosymmetric PE phase (0% displacement) is at the center, and two FE ground states are at the two ends (−100% and 100% displacements). (b) Double well potential of NbO<sub>2</sub>X monolayer along polarization direction.

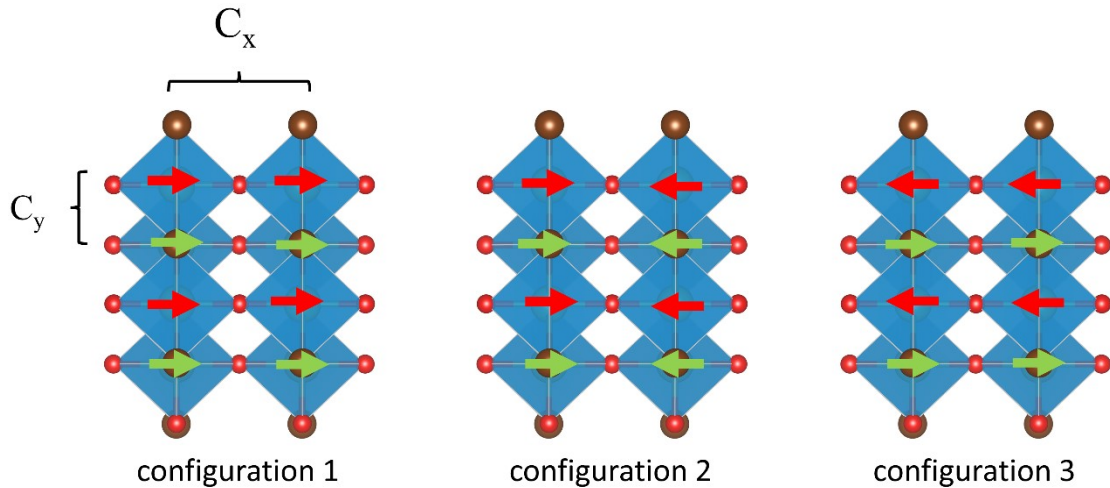


**Figure S5** Three structural configurations with different cation displacement arrangement in 2x2 supercell, are constructed to extract coefficients  $C_x$  and  $C_y$  appeared in Eq. (1). Configurations 1, 2 and 3 correspond to FE, head-to-head (tail-to-tail) and AFE polar structures, whose cation polar displacement are constrained in an exactly same magnitude. Based on Eq. (1), the normalized energy difference (per f. u.) between each structural configuration can be expressed as:  $E_2 - E_1 = 16C_x P^2$ ,  $E_3 - E_1 = 16C_y P^2$ .

**Table S1** the ground-state free energy (potential barrier)  $E_G$  (meV), the spontaneous polarization  $P_s$  ( $10^{-10}\text{C/m}$ ) at zero temperature, and fitted parameters in Eq. (1).  $A$  and  $B$  are used to describe the double-well potential.  $C$  is the constant representing the mean-field approximation interaction between the nearest neighbors. The data for SnSe and GeSe in the table is from Ref. 1.

	$E_G$	$P_s$	$A$	$B$	$C_x$	$C_y$	$T_c$
NbO <sub>2</sub> I	-82.46	3.85	-10.807	-1.528	71.35	0.92	1700
NbO <sub>2</sub> Br	-73.49	3.75	-11.259	-1.290	74.52	0.61	1500
SnSe	-3.75	1.51	-5.785	1.705	10.16	10.16	326
GeSe	-111.99	3.67	-15.869	-3.540	9.74	9.74	2300

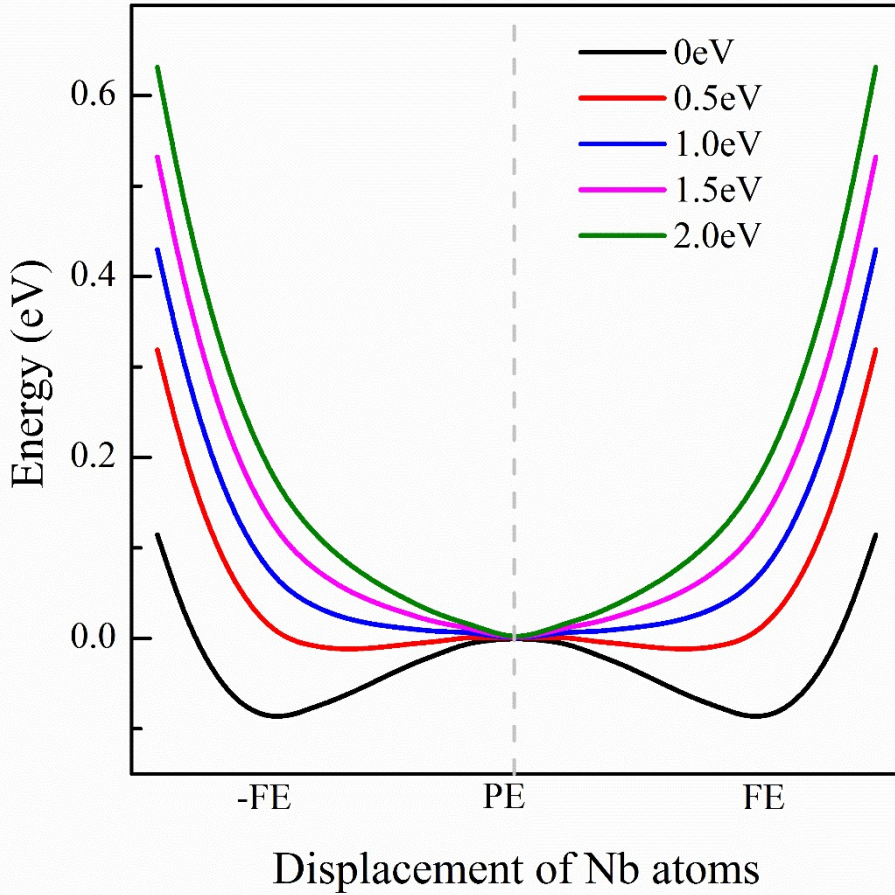


**Figure S6** The evolution of double-well as the external potential added on  $\text{Nb}^{5+}4d_{xy}/4d_{xz}$  in  $\text{NbO}_2\text{Br}$ .

**Details of OSEP method:** The spirit of the OSEP approach is to introduce a special external potential<sup>4,5</sup>. We can define a projector operator  $|inlm\sigma\rangle\langle inlm\sigma|$ , which only allows the external potential  $V_{\text{ext}}$  to influence the specific atomic orbit  $|inlm\sigma\rangle$ , in which  $i$  denotes the atomic site, and  $n, l, m, \sigma$  are the main quantum number, orbital quantum number, magnetic quantum number and spin index, respectively.

Then, we can get new Hamiltonian in OSEP method:

$$H^{\text{OSEP}} = H_{\text{KS}}^0 + |inlm\sigma\rangle\langle inlm\sigma|V_{\text{ext}} \quad (2)$$

where  $H_{\text{KS}}^0$  is the original Kohn-Sham Hamiltonian which includes all the orbital-independent potential.



### III Electronic Structure

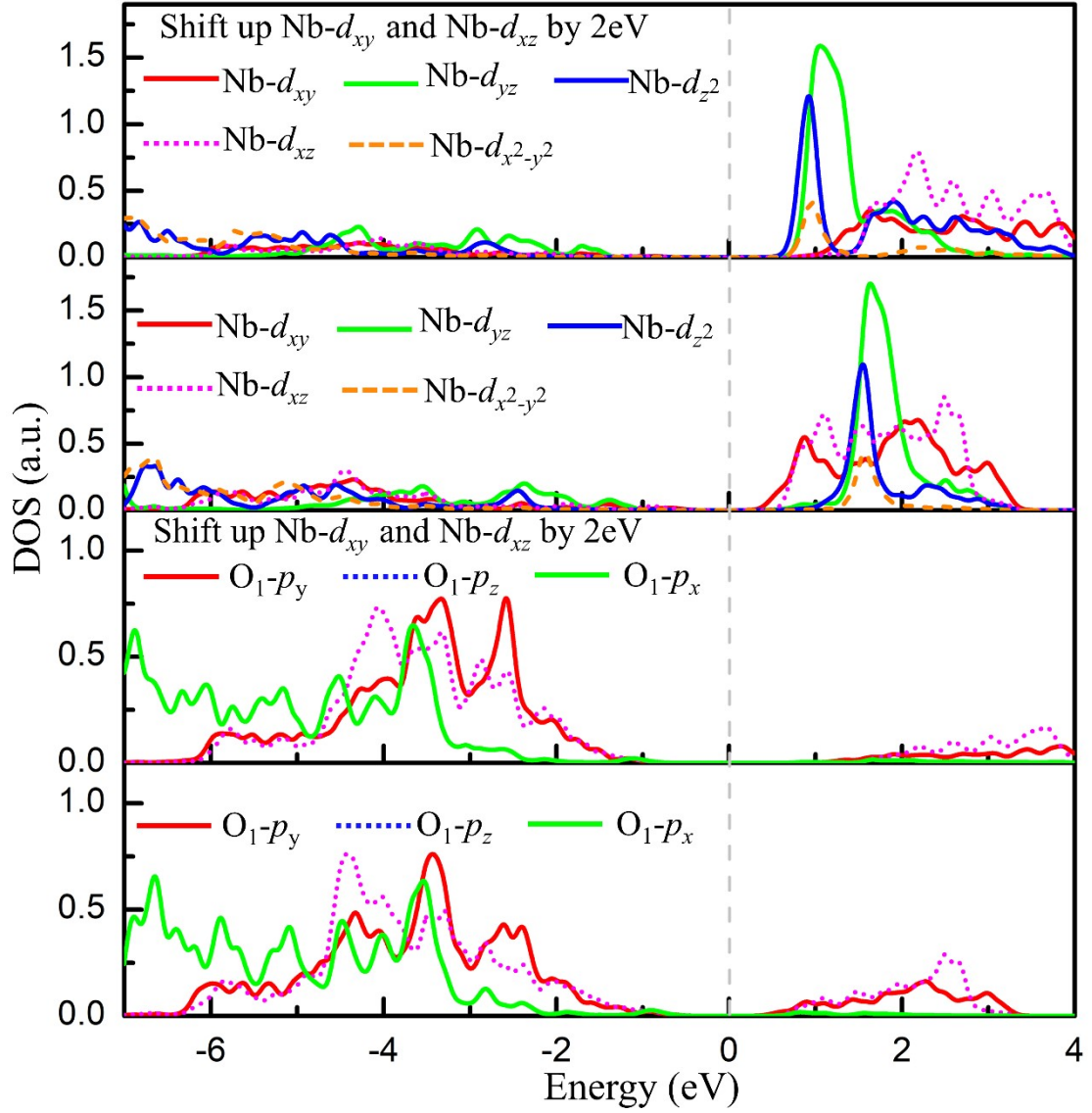


**Figure S7** the density of states of ferroelectric phase of monolayer NbO<sub>2</sub>I. (a) and (c) are calculated by applying OSEP method with an external potential as 2eV on Nb 4d<sub>xy</sub> and 4d<sub>xz</sub> to shift-up them. For comparison, we also plot out the DOS without any external potential in (b) and (d).

According to the DP theory,<sup>2,3</sup> the carrier mobility of 2D materials can be estimated by the following expression,

$$\mu_{2D} = \frac{e\hbar^3 C_{2D}}{k_B T m^* m_d E_1^2} \quad (3)$$

Where  $\hbar$  is the reduced Planck constant,  $k_B$  is Boltzmann constant, and T is the temperature (set to be 300 K).  $E_1$  denotes the deformation potential constant of holes located at the top of the valence band (VBM) or electrons clustered at the bottom of the conduction band (CBM) along the transport direction, determined by the equation  $E_1 = \Delta E / (\Delta l / l_0)$ ,  $\Delta E$  is the energy change of the CBM or VBM under compressive or tensile strain,  $l_0$  is the length of lattices in the transport direction, and  $\Delta l$  is the deformation of  $l_0$ .  $m_d$  is the average effective mass of the carriers,

defined by the equation  $m_d = \sqrt{m_x^* m_y^*}$ .  $C_{2D}$  is the elastic modulus of a uniformly deformed crystal, and for 2D materials, the elastic modulus can be determined by the equation  $C_{2D} = 2[\partial^2 E / \partial(\varepsilon)^2] / S_0$  to calculate, where  $E$  is the total energy and  $S_0$  is the optimized area.

**Table S2** calculated carrier Mobility ( $\mu$ ,  $10^3 \text{ cm}^2 \text{ V}^{-1} \text{ S}^{-1}$ ) in  $\text{NbO}_2\text{X}$  monolayers along x (polarization) and y directions at 300 K

		$m_x^*$	$m_y^*$	$E_{1x}$	$E_{1y}$	$C_{2D-x}$	$C_{2D-y}$	$\mu_x$	$\mu_y$
NbO <sub>2</sub> Br	<i>e</i>	0.39	0.61	13.32	-6.29	132.96	179.86	0.0839	0.3254
	<i>h</i>	1.02	2.83	-3.38	-0.99			0.1430	0.8729
NbO <sub>2</sub> I	<i>e</i>	0.44	1.18	11.15	-6.80	126.97	177.12	0.0686	0.0959
	<i>h</i>	0.48	1.37	-6.09	-2.09			0.1873	0.7774

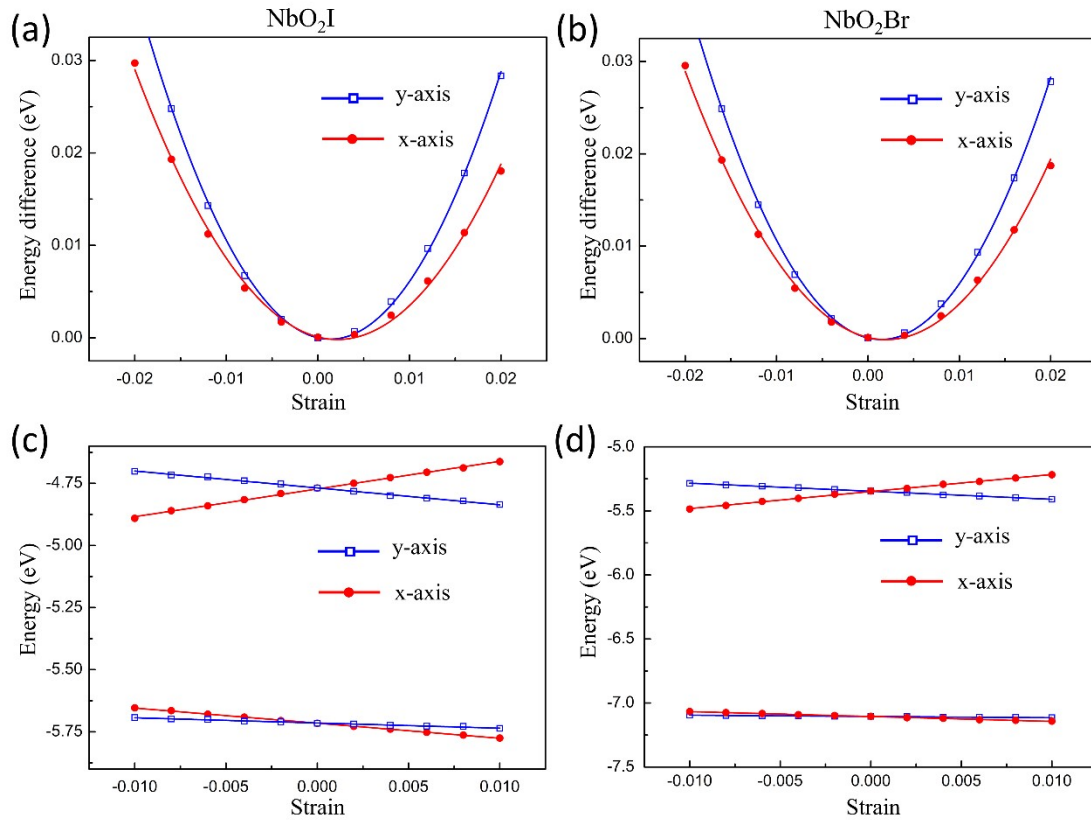


**Figure S8** Energy difference between the total energy of strained (a) NbO<sub>2</sub>I and (b) NbO<sub>2</sub>Br monolayers along the x and y directions; (c) and (d) energy shift of VBM and CBM for NbO<sub>2</sub>I and NbO<sub>2</sub>Br monolayers with respect to the lattice dilation and compression along the x and y directions, respectively.

1. R. Fei, W. Kang and L. Yang, *Physical Review Letters*, 2016, **117**, 097601.
2. J. Bardeen and W. Shockley, *Physical Review*, 1950, **80**, 72-80.
3. Y. Jing, Y. Ma, Y. Li and T. Heine, *Nano Letters*, 2017, **17**, 1833-1838.
4. X. Wan, J. Zhou, J. Dong, *EPL Europhys. Lett.* 2010, **92**, 57007;
5. Y. Du, H.-C. Ding, L. Sheng, S. Y. Savrasov, X. Wan, C.-G. Duan, *J. Phys.: Condens. Matter* 2013, **26**, 025503.

